


RESEARCH LETTER

Open Access



The 2015 M_w 6.0 Mt. Kinabalu earthquake: an infrequent fault rupture within the Crocker fault system of East Malaysia

Yu Wang^{1*} , Shengji Wei¹, Xin Wang^{1,3}, Eric O. Lindsey^{1,2}, Felix Tongkul⁴, Paul Tapponnier¹, Kyle Bradley¹, Chung-Han Chan¹, Emma M. Hill¹ and Kerry Sieh¹

Abstract

The M_w 6.0 Mt. Kinabalu earthquake of 2015 was a complete (and deadly) surprise, because it occurred well away from the nearest plate boundary in a region of very low historical seismicity. Our seismological, space geodetic, geomorphological, and field investigations show that the earthquake resulted from rupture of a northwest-dipping normal fault that did not reach the surface. Its unilateral rupture was almost directly beneath 4000-m-high Mt. Kinabalu and triggered widespread slope failures on steep mountainous slopes, which included rockfalls that killed 18 hikers. Our seismological and morphotectonic analyses suggest that the rupture occurred on a normal fault that splays upwards off of the previously identified normal Marakau fault. Our mapping of tectonic landforms reveals that these faults are part of a 200-km-long system of normal faults that traverse the eastern side of the Crocker Range, parallel to Sabah's northwestern coastline. Although the tectonic reason for this active normal fault system remains unclear, the lengths of the longest fault segments suggest that they are capable of generating magnitude 7 earthquakes. Such large earthquakes must occur very rarely, though, given the hitherto undetectable geodetic rates of active tectonic deformation across the region.

Keywords: 2015 Sabah earthquake, Mt. Kinabalu, Normal fault rupture, Teleseismic finite fault inversion, Landslides

Background

East Malaysia has a very low earthquake hazard, as it is far away from major plate boundary faults (Simons et al. 2007) (Fig. 1a). Nonetheless, infrequent earthquakes generated by intraplate active faults do occur and have caused significant damage (e.g., Lim and Godwin 1992), in part because the rarity of historical damaging earthquakes does not encourage implementation of seismic designs, preparation for earthquake-caused emergencies, and the systematic study of active faults.

Sabah is the northeastern province of East Malaysia and lies within the Sunda block, between the oceanic basins of the South China, Sulu, and Celebes Seas (Fig. 1a). The high Crocker and Trusmadi Ranges rise from Sabah's

northwestern coast. Within that mountainous backbone, by far the highest peak is Mt. Kinabalu, which consists of a granitic pluton that was rapidly exhumed since its crystallization about 5–6 Ma (Cottam et al. 2013) (Fig. 1b). These two mountain ranges are nearly parallel to an active deep-water fold-and-thrust belt that lies offshore to the northwest and has likely resulted from either gravity-driven mass movements or slow tectonic shortening (Hesse et al. 2009; King et al. 2010; Sapin et al. 2013; Simons et al. 2007). Although Sabah's active tectonic setting remains unclear, recent GPS analyses suggest that the region is moving slowly westward relative to the stable Sunda block at a rate of just a few mm/year (e.g., Simons et al. 2007; Mustafar et al. 2014). This slow convergence between Sabah and the part of the Sunda block beneath the South China Sea, together with recent geomorphic analyses implies that Sabah is dominated by contractional tectonics (e.g., Mathew et al. 2016).

*Correspondence: Y.Wang@ntu.edu.sg

¹ Earth Observatory of Singapore, Nanyang Technological University, Singapore, Singapore

Full list of author information is available at the end of the article

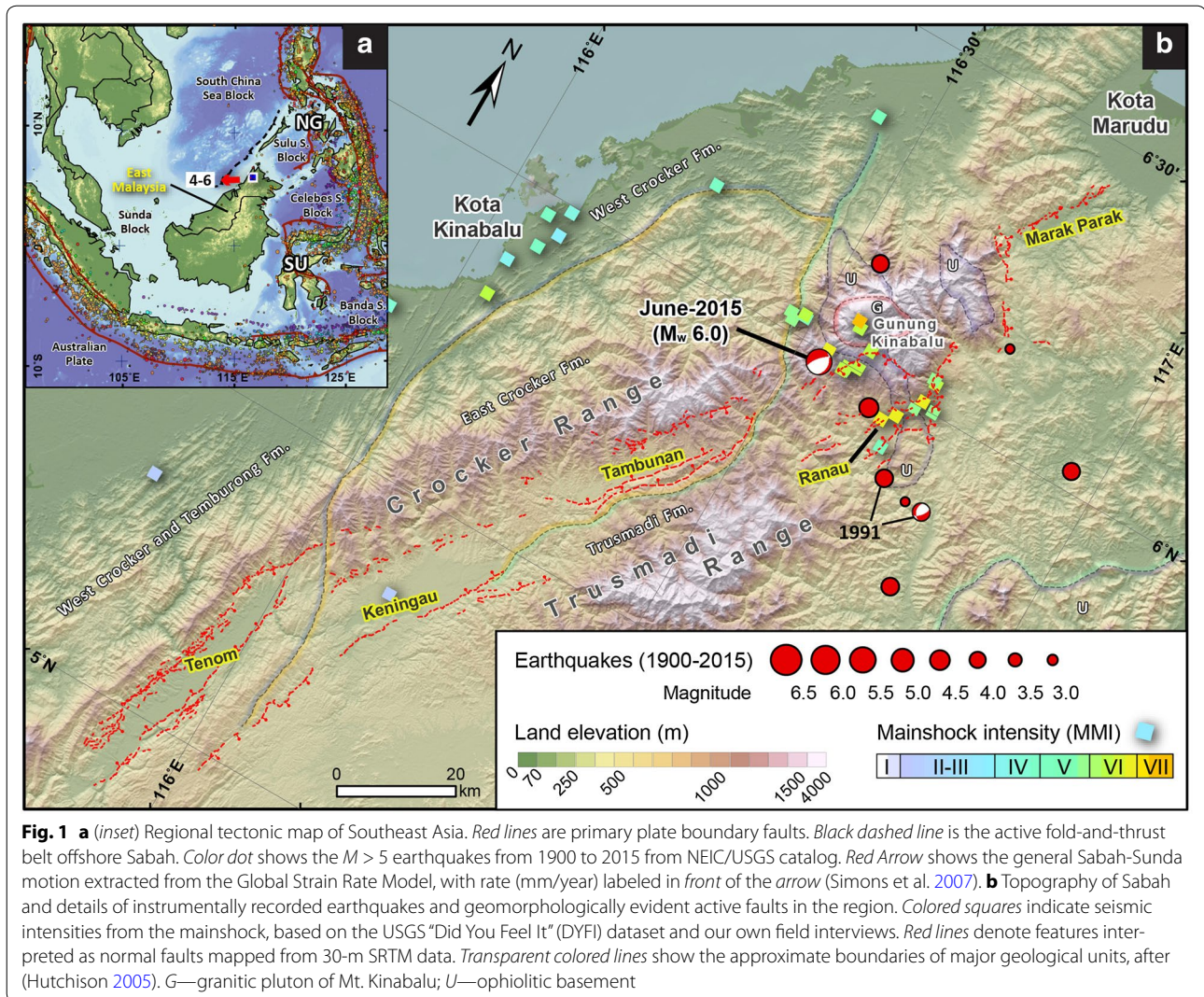


Fig. 1 **a** (inset) Regional tectonic map of Southeast Asia. Red lines are primary plate boundary faults. Black dashed line is the active fold-and-thrust belt offshore Sabah. Color dot shows the $M > 5$ earthquakes from 1900 to 2015 from NEIC/USGS catalog. Red Arrow shows the general Sabah-Sunda motion extracted from the Global Strain Rate Model, with rate (mm/year) labeled in front of the arrow (Simons et al. 2007). **b** Topography of Sabah and details of instrumentally recorded earthquakes and geomorphologically evident active faults in the region. Colored squares indicate seismic intensities from the mainshock, based on the USGS "Did You Feel It" (DYFI) dataset and our own field interviews. Red lines denote features interpreted as normal faults mapped from 30-m SRTM data. Transparent colored lines show the approximate boundaries of major geological units, after (Hutchison 2005). G—granitic pluton of Mt. Kinabalu; U—ophiolitic basement

The M_w 6.0 Mt. Kinabalu earthquake occurred at 23:15 UTC, June 4, 2015, within this ambiguous tectonic environment. It was the largest earthquake to strike Sabah province in the past century (e.g., Engdahl and Villasenor 2002) and came as a surprise to local communities. Focal mechanisms calculated by the Global Centroid-Moment-Tensor (GCMT) project and the U.S. Geological Survey (USGS/NEID) suggest the focal depth of the mainshock was between 6 and 18 km on a normal fault striking nearly N-S or NE-SW (GCMT; Ekström et al. 2012). Prior to this event, the largest recorded earthquakes were m_b 5.0 doublet in 1991 (Fig. 1b) that caused minor damage in the Ranau area, southeast of Mt. Kinabalu (Lim and Godwin 1992).

The Mt. Kinabalu mainshock produced intense ground shaking ($I_{MMI} \sim VII$) in the vicinity of Ranau town, especially in the area between the town and the summit of

Mt. Kinabalu (Fig. 1b, Additional file 1: Table S1). It also triggered extensive landslides along the steep slopes of Mt. Kinabalu, including rockfalls that killed 18 people and injured at least 21 more along climbing trails on the steep mountain face (Chan 2015). The mainshock was felt at least 300 km away, and the seismic intensity in the provincial capital, Kota Kinabalu, was strong enough ($I_{MMI} = IV$) to awaken many residents in the early morning.

This M_w 6.0 event provides a rare opportunity to improve our understanding of the seismic hazards and tectonic context of East Malaysia. Here, we combine seismology, aftershock relocations, space-based geodesy, and tectonic geomorphology to understand earthquake, to place it in an active tectonic context, and to map the extensive landslides on Mt. Kinabalu.

Point-source focal mechanism and finite fault inversion

Immediately after the M_w 6.0 mainshock, we performed a teleseismic waveform inversion to determine a moment tensor solution by the Cut-And-Paste (CAP) method (Zhu and Helmberger 1996). This yielded a normal fault mechanism similar to solutions from global seismic networks (e.g., USGS and GCMT) and a centroid depth of 13–14 km (Fig. 2a; Additional file 1: Figure S1). The 209° strike of one of the fault-plane solutions is similar to the trend of normal fault scarps that appear clearly in the nearby topography (Fig. 2b).

We also conducted a finite fault inversion using broadband teleseismic body waves with a simulated annealing inversion algorithm (Ji et al. 2002). We tested fault planes corresponding to both nodal planes of our point-source focal mechanism. Detailed inversion parameters and methods appear in the Additional file 1.

Of the two orthogonal finite fault models, the fault that strikes 209° and dips 63° fits the data much better than the more shallowly dipping fault (best waveform fits are shown in Additional file 1: Figure S2). Most of the rupture occurred at depths >5 km, and peak slip is <50 cm (Fig. 2b, c). Thus, our model predicts <3 cm of surface deformation (Additional file 1: Figure S3).

Most of the seismic energy was released in the first 5 s of the rupture process (Fig. 2d). The rupture propagated unilaterally NNE along strike and had only a small component of updip directivity. The unilateral propagation is evident in the seismic waveform records, in that the waveforms from stations located to the south show longer durations than those to the north (Fig. 2e, duration highlighted by rectangles). The northward propagation of the rupture could have increased the shaking on Mt. Kinabalu and thus have increased the likelihood of landslides and rockfalls northeast of the fault rupture.

Relocation of aftershocks

More than one hundred aftershocks were recorded by the Malaysian seismic network. However, only seven are large enough to be included in the current global catalog (e.g., USGS/NEIC). The locations of these $M \geq 4$ aftershocks differ appreciably between the USGS/NEIC and the Malaysian catalogs (Table 1; Additional file 1: Figure S4a). Since only two local stations (KKM and RNSM) within 50 km of the mainshock recorded these aftershocks, we use three-component waveform records at these two stations to relocate the aftershocks via single seismic station relocation.

To constrain aftershock locations using a single station, we estimate the backazimuth from the P-wave particle motion and the epicentral distance from the differential travel time of S- and P-wave, assuming a modified

CRUST 2.0 layered velocity structure (Bassin 2000). The backazimuth of the event is determined by rotating the N-S and E-W component records to the radial and transverse components under the guiding principle that the best angle will minimize the P-wave energy on the transverse component (Jurkevics 1988; Niu and Li 2011). The epicentral distance is determined by the differential travel time of S- and P-wave with manually picked direct P- and S-wave arrival time (Additional file 1: Figure S5). The distance is then determined by matching the differential travel time with a theoretical travel time table derived from the 1D velocity model, assuming these events are located at a depth around 13 km, which is the depth of the mainshock hypocenter (Fig. 2a).

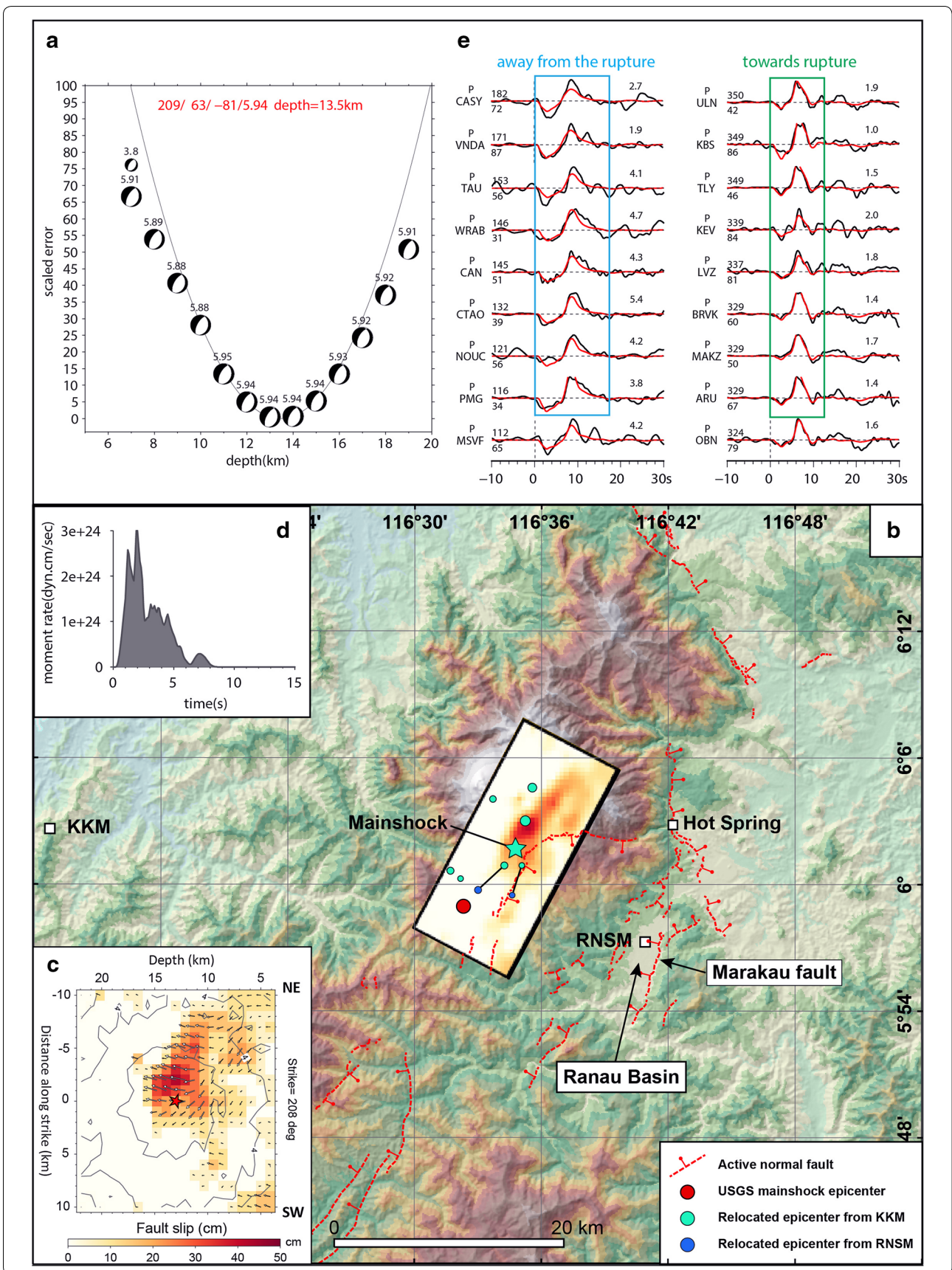
We are able to relocate the mainshock and seven aftershocks with backazimuth and distance from the single seismic station data. Two aftershocks epicenters determined from station RSNM are highly consistent with their epicenters determined from station KKM. This suggests that the single station method works well in the Mt. Kinabalu area (Fig. 2b). These eight relocated events define in a zone $\sim 15 \text{ km} \times 5 \text{ km}$, much narrower than the distribution determined without using the two local stations (Additional file 1: Figure S4). This zone is consistent with the strike of our best-fitting finite fault model and is parallel to the generalized trend of normal fault scarps mapped at the surface.

ALOS-2 observation

We use L-Band ScanSAR and stripmap data acquired by ALOS-2/PALSAR-2 to estimate surface deformation associated with the mainshock. Data from descending track 28 and ascending track 142 (Table 2) were processed using the GMTSAR software (Sandwell et al. 2011) with the application of a 100-m Gaussian filter. Overall, both ascending and descending InSAR results show surprisingly good coherence across Sabah's densely vegetated surface (Additional file 1: Figure S6).

Neither interferogram shows significant line of sight (LOS) displacement of Mt. Kinabalu, which implies that ground deformation was no more than the noise level of the interferogram, $\sim 5 \text{ cm}$ (e.g., Lin et al. 2010). This is consistent with the $\sim 3 \text{ cm}$ amplitude of surface deformation predicted from our finite fault model. Our InSAR results thus support our interpretation from the teleseismic inversion—that the earthquake resulted from a blind normal fault rupture that did not reach the surface.

While the LOS displacement fields show no appreciable tectonic ground deformation in the vicinity of Mt. Kinabalu, the interferograms contain some unusually large low-coherence patches on the slopes of Mt. Kinabalu (Fig. 3a). These may be the result of either radar overlay due to the steep topography of Mt. Kinabalu or



(See figure on previous page.)

Fig. 2 Seismological evaluation of the 2015 Kinabalu earthquake. **a** Point-source moment tensor solution from CAP analysis yields a best-fit centroid depth of about 13–14 km. **b** Map view of the finite rupture model of Mt. Kinabalu earthquake and relocated epicenters of the mainshock and select aftershocks. Upper bound of the modeled rupture plane is indicated by a heavy line, about 4 km below the surface. *Red lines* are active normal faults mapped from SRTM topography. **c** Slip in the finite rupture model, including rake angles (*white arrows*) and timing (black contours, in 2-second intervals). **d** Moment-rate function of the finite fault model shows that rupture lasted about 5 s. **e** Teleseismic P-wave fits for select stations. *Red* is synthetic and *black* is data; station names appear at the beginning of each waveform pair, as well as epicenter azimuth (above, in degrees) and distance (below, in degrees). Peak displacements (in micrometer) appear above the end of the waveform

extensive slope failures triggered by the mainshock. The latter interpretation is more viable, because these or similar low-coherence patches that do not exist in the interferogram formed from two pre-earthquake descending ALOS-2 ScanSAR images (Fig. 3b).

Landslide distribution

Inspections of post-earthquake optical Landsat 8 satellite images and photos taken in the field after the mainshock confirm that many of these low-coherence patches are either associated with large landslides and rockfalls or smaller but tightly clustered rockfalls (Fig. 3c). Both the radar interferograms and the optical imagery and photographs show that most of the slope failures occurred where the flanks of Mt. Kinabalu are steeper than 30° (Fig. 3d). Our Landsat 8 observations also indicate that some of the earthquake-induced

landslides occurred more than 30 km from the epicenter.

One of the largest of slope failures is a 6 km² patch within the river catchment on the northwestern side of Mt. Kinabalu. Another large failure is a 5 km² patch on the southern flank of Mt. Kinabalu. The match between the radar and optical interpretations is better on the northern slope than on the southern slope. This likely results from the line of sight azimuth of the ALOS-2 data, as Mt. Kinabalu's southern slope is nearly parallel to ALOS-2's line of sight, so it is more likely that not all the incoherence reflects actual changes in the slope.

The ALOS-2's descending interferogram also shows some low-coherence patches east of the Mt. Kinabalu (Fig. 3a). However, clouds obscure the optical satellite images in that region, so they cannot be used to confirm that these patches are the result of slope failures.

Table 1 Mainshock and aftershock information

Origin date (YYYYMMDD_HHMM)	Malaysia catalog				USGS catalog ^a		Relocation ^b	
	Lat.	Lon.	Dep.	Mag.	Lat.	Lon.	Lat.	Lon.
20150604_2315	6.0474	116.5900	9.0	6.0	5.9870	116.5410	6.0283	116.5798
20150605_0405	6.1256	116.4896	23.1	4.0	–	–	6.0051	116.5370
20150605_1312	6.0273	116.5569	10.0	4.2	–	–	6.0679	116.5624
20150605_1513	6.0782	116.5162	19.1	4.3	6.1400	116.7230	6.0110	116.5284
20150606_0545	6.1068	116.5644	10.0	4.8	6.1420	116.6690	6.0769	116.5931
20150612_1829	6.1013	116.6381	10.0	5.1	6.2050	116.6810	6.0505	116.5876
20150617_2158	6.0483	116.6161	10.0	4.0	–	–	6.0151 5.9918 ^c	116.5850 116.5774 ^c
20150623_0932	6.0664	116.6135	10.0	4.3	6.1280	116.5540	6.0154 5.9958 ^c	116.5714 116.5503 ^c

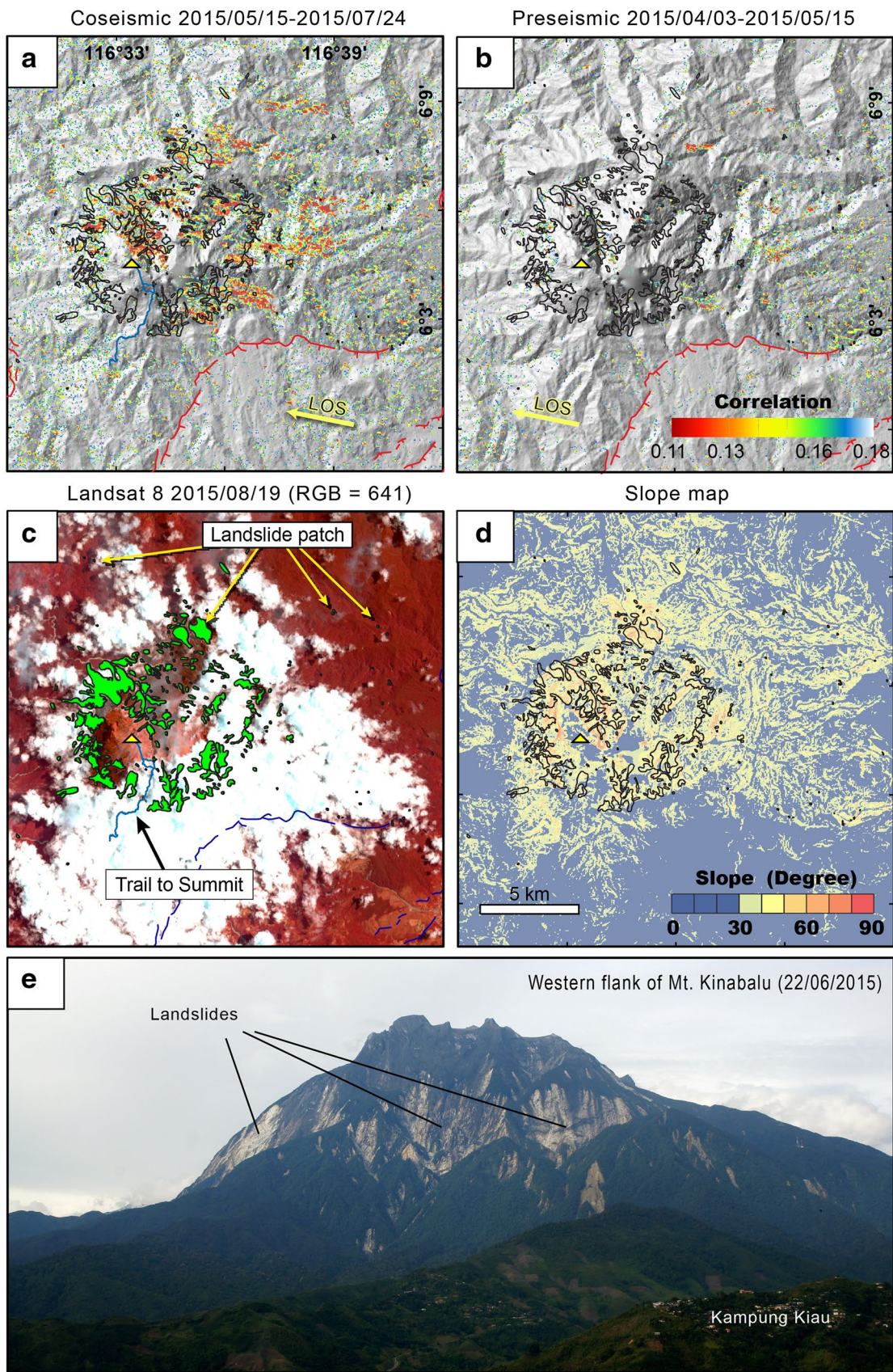
^a “–” stands for no available information from USGS website

^b Latitude and Longitude are determined from KKM station by applied bandpass filter of 50 s-1 Hz

^c Latitude and Longitude are determined from RNSM station by applied bandpass filter of 50 s-1 Hz

Table 2 ALOS-2 data used in this study

Path	Frame	Obs. Mode	Dates	Perpendicular baseline (m)	Notes
28	3500	WD1 (descending)	2015/04/03–2015/05/15	61.8	Preseismic
28	3500	WD1 (descending)	2015/05/15–2015/07/24	168.4	Coseismic
142	103	SM3 (ascending)	2015/01/19–2015/06/22	145.3	Coseismic



(See figure on previous page.)

Fig. 3 ALOS-2 coherence and slope maps show that loss of coherence is related to coseismic slope failures of slopes steeper than 30° on Mt. Kinabalu. **a** Post-seismic image correlation map of the descending tracks. Black outlines are post-seismic slope failures mapped from Landsat 8 images (*Green polygons in panel c*). *Red lines* are the active faults from this study. *Blue line* shows the trail to the summit of Mt. Kinabalu. **b** Preseismic correlation map of the same track, showing good correlation throughout the Mt. Kinabalu. **c** Landsat 8 image of Mt. Kinabalu acquired in Aug 2016 overlaid by the mapped landslides (green polygons). The area covered by could is mapped by other Landsat 8 and optical satellite images. **d** Slope map generated from SRTM data overlain with optically mapped slope failures. This map shows that slope failures caused by the earthquake correlate well with slopes steeper than 30°. **e** The western flank of Mt. Kinabalu after the Sabah earthquake. *White patches on the slope* are the new landslides areas triggered by the M_w 6.0 mainshock

Overall, the distribution of the landslides mapped from the optical imagery and InSAR roughly coincides with seismic intensities of V and higher, consistent with the global landslide–intensity relationship compiled by Keefer (1984) and Rodríguez et al. (1999). The area affected by triggered landslides is mostly within a 15×15 km (225 km^2) area near the epicenter. However, if we include other remote slope failures mapped from the post-quake Landsat 8 imagery, the total area affected by landslide is likely exceeds 500 km^2 (26×21 km). This upper-bound estimate of the landslide-affected area is slightly smaller than the 650 km^2 area affected by slope failures after the M_w 6.2 Coalinga, California, earthquake of 1983 (Rodríguez et al. 1999), but much smaller than the area of slope failures associated with North American intraplate earthquakes: The M_w 5.8 Saguenay in 1988 and the M_w 5.8 Mineral earthquake in 2011 produced slope failures regions within areas of $\sim 30,000$ to $45,000 \text{ km}^2$ (Jibson and Harp 2012; Rodríguez et al. 1999). These differences likely reflect higher attenuation of ground motion in Sabah, as the two eastern North America earthquakes were felt over an extraordinary large area due to the low seismic attenuation of eastern North American lithosphere.

The directivity of the mainshock rupture may have also affected the landslide distribution. Although nearly all the mapped large landslides occurred on slopes of Mt. Kinabalu that average $>30^\circ$, smaller landslides occurred primarily north of the mainshock epicenter, and few occurred on the steep slopes south of Mt. Kinabalu. This is consistent with the rupture propagation direction determined by our finite fault inversion (Fig. 3c). We hypothesize that the unilateral rupture enhanced ground shaking north of Mt. Kinabalu and whereby triggered relatively extensive small landslides north of the mainshock epicenter and few to the south.

Active normal faults in northwestern Sabah

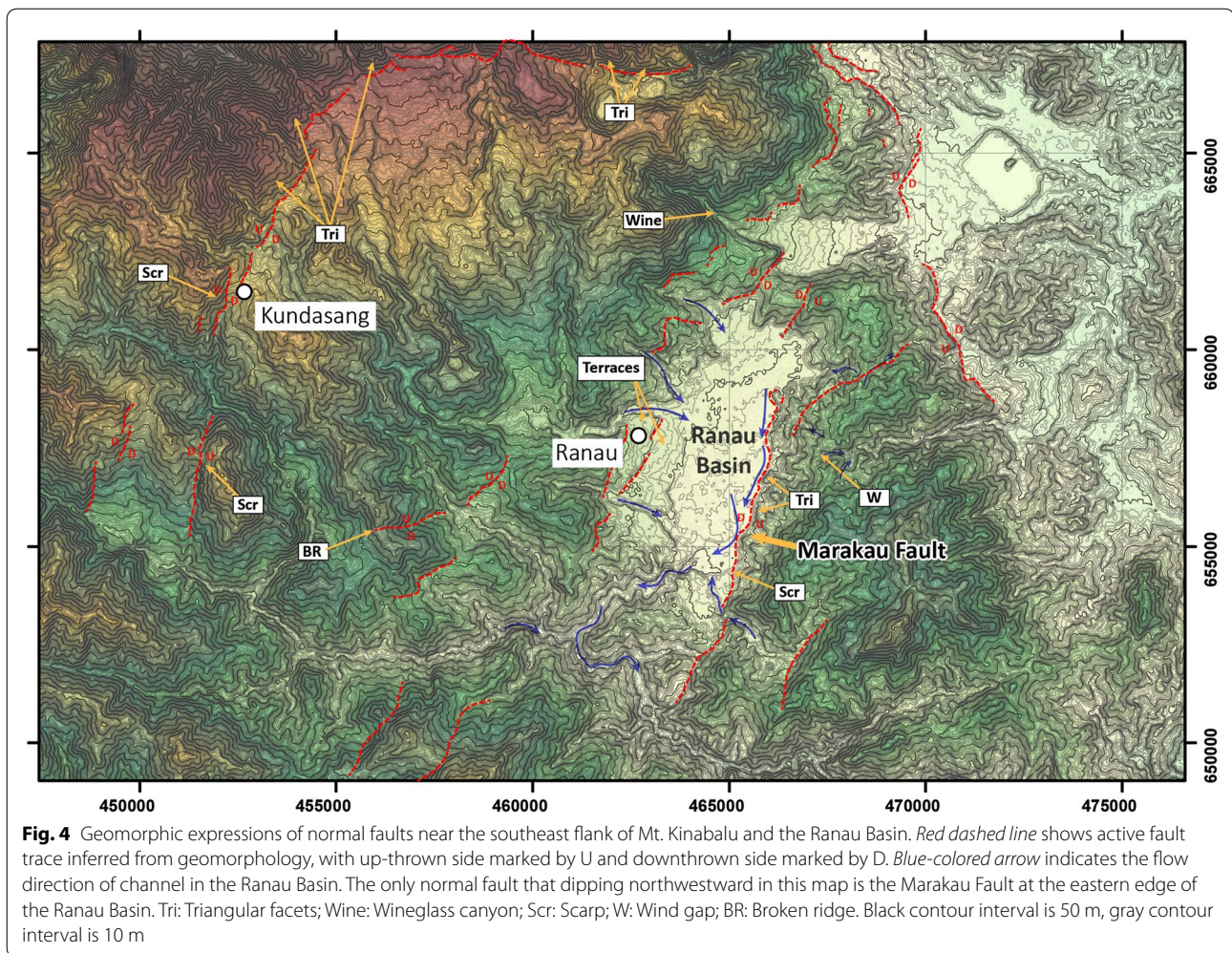
The occurrence of the Sabah earthquake motivated us to inspect the mountainous terrain for geomorphological evidence of youthful tectonic deformation. Not only did we inspect the immediate region of the earthquake for evidence of coseismic fault rupture, but we also

examined the surrounding region for evidence of active faults, to see if the location and mechanism of the earthquake could be related to a larger system of tectonic elements. Shaded relief and 10-m contour maps made from the 30-m SRTM global dataset enabled and greatly facilitated these local and regional inspections.

The topography of Sabah bears clear evidence for a 200-km-long system of active normal faults that extend northeast to southwest, through the epicentral region (Fig. 1b). The scarps of these normal faults bound five discrete valleys and exhibit hundreds of meters of topographic relief between the valley floors and mountain crests. The topographic evidence for youthful normal faulting along these valley margins is typical—triangular facets, scarps across alluvial terraces and other topographic truncations best explained by normal faulting (Additional file 1: Figures S7, S8). These geomorphic interpretations of normal faulting are consistent with the field observations of Tjia (2007) who describes normal faulting of Quaternary sediments within this fault system.

We name this the Crocker fault system, because the Crocker Range extends along nearly half its length. It divides naturally into a set of five distinct graben and master faults, one associated with each of the Tenom, Keningau, Tambunan, Ranau, and Marak Parak valleys (Fig. 1b). Lengths of individual graben and associated fault zones range from about 20 to about 60 km. Four of these appear to be half-graben, in that they exhibit only one bounding fault or one of the bounding faults is dominant over the other. Of these four, two have dominant faults that dip southeast and the other two have dominant faults dipping northwest. The three grabens southwest of Mt. Kinabalu comprise about 120 km of the entire system, and the width of the system ranges from 10 to 20 km. The half-graben northeast of Mt. Kinabalu exhibits a single, narrow fault that dips southeast. -Mt. Kinabalu clearly interferes with the regularity of the Crocker fault system, and the faulting immediately to the NE and SW and on the southern flank of the mountain is complex, with a variety of fault orientations and faults with opposing dips.

In particular, faulting near the mainshock epicenter is complex (Figs. 2a, 4). Two SE-dipping normal faults are



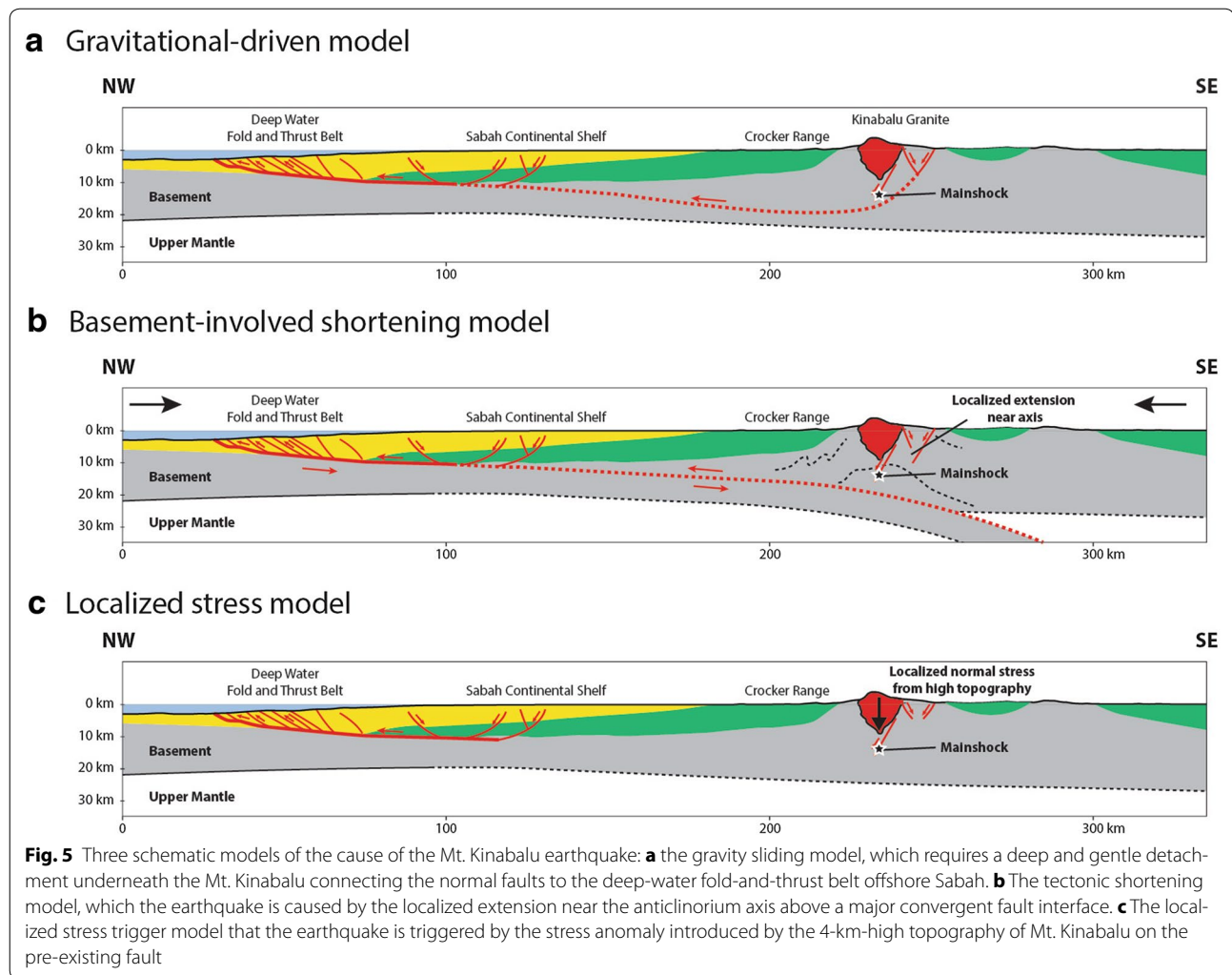
exposed along the eastern and the southern flank of Mt. Kinabalu, but the ~10-km-long, west-dipping Marakau Fault bounds the eastern margin of the Ranau basin (Fig. 2a). Mapping of triangular facets and field observations suggest that the Marakau Fault truncates the Trusmadi formation (Figs. 1, 4). Streams within the Ranau basin systemically flow eastward until they reach the eastern margin of the basin, and fluvial terraces are well developed along the western margin of the basin (Fig. 4). These observations suggest that eastward tilt of its hangingwall block has accompanied late-Quaternary motion of the west-dipping Marakau fault.

The Mt. Kinabalu earthquake likely resulted from the rupture of the northwest-dipping Marakau fault or a closely associated fault beneath Mt. Kinabalu. Of the faults we see in the topography, the Marakau fault is the only plausible source of the earthquake. The fault trace lies about 16 km southeast of the epicenter and has a strike and dip that is similar to that of the earthquake's focal mechanism. However, if our hypocenter of the

earthquake is correct, the Marakau fault cannot actually be the source of the earthquake, because the Marakau fault would need to have an average surface-to-hypocentral dip of only 40°, far shallower than the 60° dip we determined for the rupture. Moving the earthquake epicenter about 8 km toward the Marakau fault would allow the requisite 60° dip, but 8 km is well beyond the ~3 km uncertainty of our epicentral estimation. We therefore contend that the earthquake resulted from failure of a minor fault that splays upward from the Marakau Fault and does not break the surface.

Tectonic implications

The tectonic implications of the Mt. Kinabalu earthquake and the Crocker fault system remain uncertain. While the normal fault mechanism and the geometry of the regional fault system indicate crustal extension perpendicular to the coast of Sabah, offshore structures clearly show ongoing shortening (e.g., Ingram et al. 2004; Hesse et al. 2009). Moreover, the earthquake and the Crocker



fault system imply subsidence of Mt. Kinabalu, whereas geological evidence indicates that the Mt. Kinabalu Granite has risen rapidly since its crystallization 5–6 Ma (Cottam et al. 2013). These contradictions suggest that the extensional forces that are creating the normal fault system are directly related neither to the forces creating the offshore fold-and-thrust belt nor to those that have created the edifice of Mt. Kinabalu.

Previous studies have suggested that northwestern Sabah is collapsing northwestward into the South China Sea by gravitational collapse, as a gigantic landslide (e.g., Sapin et al. 2013; Sandal 1996). Ostensibly, the Crocker fault system could be the extensional headscarp of this gigantic landslide (Fig. 5a). However, the 13- to 14-km hypocentral depth of the Mt. Kinabalu rupture is far too deep and its 60° dip far too steep to lend support to this hypothesis. Normal faulting associated with a great landslide would need to occur at far shallower depths, above the low-angle detachment fault that would connect the offshore fold-and-thrust belt with the normal faults of

the headscarp. Such faults on the Niger Delta, for example, occur at depths ≤ 10 km (Corredor et al. 2005).

Alternatively, we could hypothesize that the normal faults of the Crocker fault system are the manifestation of extension at the crest of an anticlinorium that is forming above a deep, convex-upward thrust fault that farther updip is producing the offshore fold-and-thrust belt (Fig. 5b). If so, then northern Sabah might be experiencing basement-involved tectonic shortening, as suggested by Hesse et al. (2009).

Another hypothesis is that the earthquake was triggered by localized stresses associated with the topographic prominence of 4000-m high Mt. Kinabalu above the surrounding landscape (Fig. 5c). In such a case, the rupture would have reactivated a pre-existing normal fault beneath the mountain (e.g., Lin 2005). This hypothesis might suffice to explain the earthquake, but it would not explain the regional extent of the active Crocker fault system and other normal mechanism seismicity in Sabah outside the Mt. Kinabalu region.

The 13- to 14-km depth of the Mt. Kinabalu earthquake and the 200 km length of the Crocker fault system lead us to prefer the hypothesis that this narrow extensional fault system is part of a deeper tectonically driven convergent system that verges toward the offshore fold-and-thrust belt. Further tests of the hypothesis could include comparison of the modern rates of convergence and extension across the offshore and onshore zones of convergence and extension, and geophysical analysis of the crustal-scale structural geometry of northwestern Sabah.

The potential for larger earthquakes within the Crocker fault system

The presence of youthful, geomorphically expressed normal faults well beyond the source of the Mt. Kinabalu rupture implies that future seismic ruptures are plausible well beyond the region of the 2015 earthquake. It also implies that past and future ruptures could be larger than the 2015 rupture. Indeed, the 40- to 60-km lengths of the larger faults within the Crocker fault system suggest that M_w 7+ earthquakes are plausible anywhere along the 200-km-long belt (cf. the length–magnitude relationships of Wells and Coppersmith 1994; Wesnousky 2008; Blaser et al. 2010).

The recurrence intervals of such large events are, however, likely to be at least several thousand years, as the geological slip rates of these faults are likely lower than 1 mm/year (e.g., Mustafar et al. 2014). To explore plausible earthquake recurrence times for the Crocker fault system as a whole, we conduct a simple earthquake frequency model using the relationship between average fault slip rate (R) and seismic-moment accumulation rate (\dot{M}_0):

$$\dot{M}_0 = \mu \left(L \frac{W}{\sin(d)} \right) R \quad (1)$$

and

$$M_w = \frac{2}{3} \log_{10} M_0 - 10.73; \quad M_0 \text{ in dyne} \cdot \text{cm} \quad (2)$$

for which we assume a uniform 0.5 mm/year fault slip rate (R) across a fault with aggregate length (L) of 300 km, allowing for additional length from overlaps and splays within Crocker fault system, a seismogenic depth (W) of 15 km and a dip (d) of 70°. We also assume that the frequency of larger earthquakes along this normal fault system follows the truncated Gutenberg–Richter relationship:

$$\log_{10} N(M_w) = a - bM_w; \quad M_w \leq M_{\text{Max}} \quad (3)$$

where northern Sabah has a b value of 0.9, and maximum magnitude about M_w 7.3 (M_{Max}) from the empirical *fault length–magnitude* relationship (e.g., Wells and

Coppersmith 1994). With an average crustal rigidity (μ) of 3×10^{11} dyne/cm², this model yields a frequency for magnitudes ≥ 5 of about 20 years, for magnitudes ≥ 6 of nearly 150 years, and for magnitudes ≥ 7 of about 1300 years. This roughly coincides with actual earthquake frequencies for the Sabah region, as seen in the global catalog of earthquakes since 1900—five magnitude ≥ 5 events from 1900 to 2015 and the lone magnitude 6 of 2015.

If we assume a much lower fault slip rate—only 0.1 mm/year—then a magnitude ≥ 7 earthquake would be expected far less frequently—about every 6300 years. An accurate measurement of geodetic strains across the region or paleoseismic investigations might enable determination of which of these two estimates is closer to reality. Such knowledge could be quite important, because destructive strong ground motions from a $M7+$ earthquake could extend well beyond nearby towns and villages, to even as far as Sabah's capital city, Kota Kinabalu, which currently has a population of over 500,000 people.

If the Crocker fault system is the expression of a bending-moment fault above a tectonically driven thrust fault that verges into Sabah's offshore faults, the potential for even larger earthquakes sourced from the underlying thrust fault would exist. This connection is so speculative, however, that we do not consider scenarios for such earthquakes.

Even if large earthquakes occur within the Crocker fault system only every few thousand years, prudence dictates that preparations for such events take place. Many of Earth's most recent seismic disasters have resulted from the rupture of faults that have recurrence times measured in thousands of years. The average recurrence interval of the Longmenshan Fault that produced the M_w 7.9 Wenchuan earthquake in 2008 may well be 3–4 kyear (e.g., Ran et al. 2013; Ren and Zhang 2013). The Greendale Fault, which produced the 2010 M_w 7.1 Darfield earthquake, has a mean recurrence interval of 10–60 kyear (Hornblow et al. 2014). In both of these examples, the average fault slip rate of the source faults has been difficult to estimate using modern geodetic data because they are so low. Thus, as in the case of Sabah, these faults drew scant or no attention before their devastating earthquakes.

The implication of future seismic hazard analysis of Southeast Asia

The Sabah earthquake should also raise concerns about seismic potential of some Southeast Asian regions beyond East Malaysia, as very low slip rate faults are not limited to the Sabah region. Several other places in Southeast Asia with slowly slipping faults may also experience a similar level of the seismic hazard. Parts of

peninsular Malaysia, and western and southwestern Thailand also exhibit evidence of active low slip rate faults or other evidence of recent tectonic movement (e.g., Fenton and Sutiwanich 2005; Pananont et al. 2011; Tjia 2010; Shuib 2011). Geodetic analyses within the past several decades suggest that ongoing tectonic strain accumulation in these regions is lower than can yet be resolved by space-based geodesy (i.e., less than a few mm/year). Nonetheless, recent seismic activity or the geological investigations in these regions suggests a potential for future damaging earthquakes. Although the average frequency of large, destructive earthquakes in these regions may—as in the case of Sabah—be low, rapid economic development and population growth have significantly increased their seismic risk. Vigorous efforts to quantify the seismic hazards and risks of Sabah and these other areas would be an important first step toward mitigating the potentially tragic effects of future earthquakes.

Conclusions

Our teleseismic waveform and finite fault inversion results suggest the M_w 6.0 Mt. Kinabalu earthquake resulted from rupture of a blind, northwest-dipping normal fault that likely splay upward from the Marakau fault, which reaches the surface on the east side of the Ranau Valley. The maximum coseismic slip revealed by our finite fault model is <50 cm and at a depth of 13–14 km. This blind rupture area is consistent with aftershock relocations and agrees with our field and ALOS-2 InSAR observations of no appreciable surface deformation or surface rupture near Mt. Kinabalu. The landslides mapped from the optical satellite imagery and ALOS-2 InSAR together suggest the area affected by landslides is >225 km², and may be as large as 500 km². This area coincides roughly with the region of seismic intensities V and higher and with slopes exceeding 30°. The unilateral rupture of the mainshock likely enhanced the ground shaking in the area north of Mt. Kinabalu and triggered more landslides north of the mainshock epicenter than to the south.

Our geomorphological analysis indicates that the fault that caused the M_w 6.0 earthquake is part of the 200-km-long Crocker fault system, which follows the backbone of the Crocker Range. Although the tectonic significance of this narrow fault system is unclear, its scale implies that future seismic ruptures well beyond the region of the 2015 earthquake are plausible, and that this fault system may be capable of producing a magnitude ≥ 7 earthquake. Like other active faults with low slip rate, the recurrence interval of such large earthquakes along the Crocker fault system is likely to be in the order of several thousand years. However, the destructive strong ground motions from a M7+ earthquake could extend well beyond nearby towns and villages, and could bring significant

seismic hazard to Sabah's coastal settlements, including its capital city, Kota Kinabalu.

Additional file

Additional file 1. Additional figures and table.

Authors' contributions

YW performed the landslide analysis from optical imagery, field survey, interviews, and organized the paper. KS and YW conducted the active fault mapping of Sabah from remote sensing data. SW and XW performed the seismological analysis and aftershock relocations. PT provided his insight of active tectonic model of Sabah, which forms one of the major part of our discussion. EOL did the ALOS-2 InSAR analysis. FT, PT contributed extensively to the scientific discussion and data acquisition. PT, KB, and EMH shared their knowledge of this event and regional tectonics. CHC performed the seismic catalog analysis of Sabah. All authors read and approved the final manuscript.

Author details

¹ Earth Observatory of Singapore, Nanyang Technological University, Singapore, Singapore. ² Institute of Geophysics and Planetary Physics, Scripps Institution of Oceanography, University of California, San Diego, CA, USA. ³ Key Laboratory of Earth and Planetary Physics, Institute of Geology and Geophysics, Chinese Academy of Sciences, Beijing, People's Republic of China. ⁴ Natural Disaster Research Centre, Universiti Malaysia Sabah, Kota Kinabalu, Sabah, Malaysia.

Acknowledgements

We deeply appreciate the help from Dr. Rosaidi Che Abas from the Malaysian Meteorological Department (MetMalaysia), who provided the raw data of local seismic stations for earthquake relocations. We also greatly appreciate the help of Yvonne Soon Yee Yun in conducting our field work. ALOS-2 data are copyrighted by the Japanese Aerospace Exploration Agency. This research is supported by the National Research Foundation Singapore and the Singapore Ministry of Education under the Research Centres of Excellence initiative. This work comprises Earth Observatory of Singapore contribution no. 143.

Competing interests

The authors declare that they have no competing interests.

Received: 13 October 2016 Accepted: 21 February 2017

Published online: 09 March 2017

References

- Bassin C (2000) The current limits of resolution for surface wave tomography in North America. *EOS Trans AGU* 81:F897
- Blaser L, Kruger F, Ohrnberger M, Scherbaum F (2010) Scaling relations of earthquake source parameter estimates with special focus on subduction environment. *Bull Seismol Soc Am* 100(6):2914–2926. doi:10.1785/0120100111
- Chan J (2015) All earthquake victims accounted for, Sabah cops confirm. *The Malay Mail Online*, Jun 10, 2015
- Corredor F, Shaw JH, Bilotti F (2005) Structural styles in the deep-water fold and thrust belts of the Niger Delta. *AAPG Bull* 89(6):753–780. doi:10.1306/02170504074
- Cottam MA, Hall R, Sperber C, Kohn BP, Forster MA, Batt GE (2013) Neogene rock uplift and erosion in northern Borneo: evidence from the Kinabalu granite, Mount Kinabalu. *J Geol Soc* 170(5):805–816. doi:10.1144/jgs2011-130
- Ekström G, Nettles M, Dziewoński AM (2012) The global CMT project 2004–2010: centroid-moment tensors for 13,017 earthquakes. *Phys Earth Planet Inter* 200–201:1–9. doi:10.1016/j.pepi.2012.04.002
- Engdahl E, Villasenor A (2002) Global seismicity: 1900–1999, international handbook of earthquake and engineering seismology 81A. Elsevier Science Ltd, Amsterdam

- Fenton C, Sutiwanich C (2005) Paleoseismic investigation of the Ranong and Khlong Marui faults, Chumphon Province, Southern Thailand. In: AGU Fall Meeting Abstracts
- Hesse S, Back S, Franke D (2009) The deep-water fold-and-thrust belt offshore NW Borneo: gravity-driven versus basement-driven shortening. *Geol Soc Am Bull* 121(5–6):939–953. doi:10.1130/b26411.1
- Hornblow S, Quigley M, Nicol A, Van Dissen R, Wang N (2014) Paleoseismology of the 2010 M_w 7.1 Darfield (Canterbury) earthquake source, Greendale Fault, New Zealand. *Tectonophysics* 637:178–190. doi:10.1016/j.tecto.2014.10.004
- Hutchison CS (2005) *Geology of north-west Borneo: Sarawak, Brunei and Sabah*. Elsevier, Amsterdam. ISBN: 9780080460895
- Ingram GM, Chisholm TJ, Grant CJ, Hedlund CA, Stuart-Smith P, Teasdale J (2004) Deepwater North West Borneo: hydrocarbon accumulation in an active fold and thrust belt. *Mar Pet Geol* 21(7):879–887. doi:10.1016/j.marpetgeo.2003.12.007
- Ji C, Wald DJ, Helmberger DV (2002) Source description of the 1999 Hector Mine, California, earthquake, part I: wavelet domain inversion theory and resolution analysis. *Bull Seismol Soc Am* 92(4):1192–1207. doi:10.1785/0120000916
- Jibson RW, Harp EL (2012) Extraordinary distance limits of landslides triggered by the 2011 Mineral, Virginia, earthquake. *Bull Seismol Soc Am* 102(6):2368–2377
- Jurkevics A (1988) Polarization analysis of three-component array data. *Bull Seismol Soc Am* 78(5):1725–1743
- Keefer DK (1984) Landslides caused by earthquakes. *Geol Soc Am Bull* 95(4):406–421. doi:10.1130/0016-7606(1984)95<406:lcb>2.0.co;2
- King RC, Backé G, Morley CK, Hillis RR, Tingay MRP (2010) Balancing deformation in NW Borneo: quantifying plate-scale vs. gravitational tectonics in a delta and deepwater fold-thrust belt system. *Mar Pet Geol* 27(1):238–246. doi:10.1016/j.marpetgeo.2009.07.008
- Lim P, Godwin P (1992) The Ranau Earthquake Swarm, May–July, 1991, Sabah
- Lin CH (2005) Seismicity increase after the construction of the world's tallest building: an active blind fault beneath the Taipei 101. *Geophys Res Lett* 32:L22313. doi:10.1029/2005GL024223
- Lin Y-N, Simons M, Hetland EA, Muse P, DiCaprio C (2010) A multiscale approach to estimating topographically correlated propagation delays in radar interferograms. *Geochem Geophys Geosyst*. doi:10.1029/2010GC003228
- Mathew MJ, Menier D, Siddiqui N, Kumar SG, Authemayou C (2016) Active tectonic deformation along rejuvenated faults in tropical Borneo: inferences obtained from tectono-geomorphic evaluation. *Geomorphology* 267:1–15
- Mustafar MA, Simons WJ, Omar KM (2014) Monitoring of local deformations in North Borneo. Paper presented at the FIG Congress 2014, Kuala Lumpur
- Niu F, Li J (2011) Component azimuths of the CEArray stations estimated from P-wave particle motion. *Earthq Sci* 24(1):3–13. doi:10.1007/s11589-011-0764-8
- Pananont P, Wechbunthung B, Putthapiban P, Wattanadilokkul D (2011) Seismic activities in Kanchanaburi: past and present. *Songklanakarin J Sci Technol* 33(3):355–364
- Ran Y-K, Chen W-S, Xu X-W, Chen L-C, Wang H, Yang C-C, Dong S-P (2013) Paleoseismic events and recurrence interval along the Beichuan-Yingxiu fault of Longmenshan fault zone, Yingxiu, Sichuan, China. *Tectonophysics* 584:81–90. doi:10.1016/j.tecto.2012.07.013
- Ren J, Zhang S (2013) Estimation of recurrence interval of large earthquakes on the Central Longmen Shan fault zone based on seismic moment accumulation/release model. *Sci World J* 2013:8. doi:10.1155/2013/458341
- Rodriguez CE, Bommer JJ, Chandler RJ (1999) Earthquake-induced landslides: 1980–1997. *Soil Dyn Earthq Eng* 18(5):325–346. doi:10.1016/S0267-7261(99)00012-3
- Sandal ST (1996) The geology and hydrocarbon resources of Negara Brunei Darussalam. Syabas, Selangor
- Sandwell D, Mellors R, Tong X, Wei M, Wessel P (2011) Open radar interferometry software for mapping surface Deformation. *EOS Trans Am Geophys Union* 92(28):234. doi:10.1029/2011EO280002
- Sapin F, Hermawan I, Pubellier M, Vigny C, Ringenbach J-C (2013) The recent convergence on the NW Borneo Wedge—a crustal-scale gravity gliding evidenced from GPS. *Geophys J Int* 193(2):549–556. doi:10.1093/gji/ggt054
- Shuib MK (2011) Evidences for recent seismicities and dating of active faulting in NW Peninsular Malaysia. In: National geoscience conference 2011, Johor Bahru, p 64
- Simons WJF, Socquet A, Vigny C, Ambrosius BAC, Haji Abu S, Promthong C, Subarya C, Sarsito DA, Matheussen S, Morgan P, Spakman W (2007) A decade of GPS in Southeast Asia: resolving Sundaland motion and boundaries. *J Geophys Res Solid Earth* 112(B6):B06420. doi:10.1029/2005JB003868
- Tjia H (2007) Kudasang (Sabah) at the intersection of regional fault zones of Quaternary age. *Geol Soc Malaysia Bull* 53:59–66
- Tjia H (2010) Growing evidences of active deformation in the malay basin region. *Geol Soc Malaysia Bull* 56:35–40
- Wells DL, Coppersmith KJ (1994) New empirical relationships among magnitude, rupture length, rupture width, rupture area, and surface displacement. *Bull Seismol Soc Am* 84(4):974–1002
- Wesnously SG (2008) Displacement and geometrical characteristics of earthquake surface ruptures: issues and Implications for seismic-hazard analysis and the process of earthquake rupture. *Bull Seismol Soc Am* 98(4):1609–1632. doi:10.1785/0120070111
- Zhu LP, Helmberger DV (1996) Advancement in source estimation techniques using broadband regional seismograms. *Bull Seismol Soc Am* 86(5):1634–1641

Submit your manuscript to a SpringerOpen® journal and benefit from:

- Convenient online submission
- Rigorous peer review
- Immediate publication on acceptance
- Open access: articles freely available online
- High visibility within the field
- Retaining the copyright to your article

Submit your next manuscript at ► springeropen.com